Test for Cosmological Parity Violation Using the 3D Distribution of Galaxies

Robert N. Cahn [*]
Lawrence Berkeley National Laboratory, 1 Cyclotron Road, Berkeley, California 94720, USA

Zachary Slepian and Jiamin Hou
Department of Astronomy, University of Florida, 211 Bryant Space Science Center, Gainesville, Florida 32611, USA and Max-Planck-Institut für Extraterrestische Physik, Postfach 1312, Giessenbachstr., 85748 Garching, Germany

(Received 28 October 2021; revised 7 January 2023; accepted 10 April 2023; published 19 May 2023)

We show how the galaxy four-point correlation function can test for cosmological parity violation. The detection of cosmological parity violation would reflect previously unknown forces present at the earliest moments of the Universe. Recent developments both in rapidly evaluating galaxy N-point correlation functions and in determining the corresponding covariance matrices make the search for parity violation in the four-point correlation function possible in current and upcoming surveys such as those undertaken by Dark Energy Spectroscopic Instrument, the *Euclid* satellite, and the Vera C. Rubin Observatory. We estimate the limits on cosmic parity violation that could be set with these data.

DOI: 10.1103/PhysRevLett.130.201002

Introduction.—Among the known fundamental forces, only the weak interaction violates parity [1–3]. Since the weak interaction played no role in the evolution of the large-scale distribution of matter, observation of cosmological parity violation would imply the existence of new forces at the time of inflation. The Sakharov conditions [4] for producing the baryon-antibaryon asymmetry (see, e.g., Ref. [5] for a review) require violations of both charge conjugation invariance (C) and of CP, the combination of C with parity (P). The weak interactions violate CP as well as parity [6], but this is well described by the standard model of particle physics and cannot account for the observed baryon-antibaryon asymmetry. Whatever new CP-violating force is responsible for the asymmetry may violate parity as well.

Searches for parity violation have a long history. In 1848, Pasteur directly observed a parity asymmetry. He found that artificially synthesized tartaric acid crystals could be separated into two distinct groups by their shapes. The crystals in one group were mirror images of those in the other group. However, tartaric acid produced organically in grapes yielded crystals of only one group. This occurred because organic molecules contain tetravalent carbon and when the carbon atom is attached to four different atoms the result is a tetrahedral shape that is distinguishable from its mirror image. That our hearts are on the left side of the body must owe its ultimate origin to the presence of just one form of each amino acid and the absence of its mirror image. Indeed, looking for dominance of organic molecules with a single chirality has been used in searches for extraterrestrial life (see, e.g., Ref. [7] for a review).

In this Letter, we present a novel means of testing parity invariance in 3D large-scale structure, relying on the same principle as Pasteur's original separation: in general, in 3D a tetrahedron and its mirror image cannot be superimposed.

The possibility of parity violation in large-scale structure is independent of homogeneity and isotropy: a large jar of crystals of one of the forms of tartaric acid would be homogeneous and isotropic to the extent of its volume. On the other hand, parity violation in 3D detected in the four-point correlation function (4PCF) would be evidence for primordial non-Gaussianity, since the 4PCF produced by a purely Gaussian random field would be simply products of 2PCFs and hence parity-conserving. In addition, the technique described here can be used to search for parity violation in a straightforward way in five-point and higher correlation functions using the algebraic structures described in Ref. [8].

Tests of parity invariance in the cosmic microwave background have been discussed for more than two decades [9–16] and carried out in Ref. [17]. Parity violation might be observable, as well, in primordial gravity waves [18]. Our proposal opens the search to an entirely new class of experiments: 3D large-scale structure surveys.

Possible sources of cosmological parity violation.—Two frequently considered potential sources of cosmological parity violation are represented by the Lagrangian densities

$$\mathcal{L} \propto \phi F^{\mu\nu}\tilde{F}_{\mu\nu} \tag{1}$$

and

$$\mathcal{L} \propto \phi R^{\mu\nu\sigma\lambda}\tilde{R}_{\mu\nu\sigma\lambda}. \tag{2}$$

In Eq. (1), $F^{\mu\nu}$ is the field strength of an Abelian field like that associated with electromagnetism [9,19] and $\tilde{F}_{\mu\nu} = \epsilon_{\mu\nu\alpha\beta}F^{\alpha\beta}$ is its dual field, with $\epsilon_{\mu\nu\alpha\beta}$ denoting the

Levi-Civita tensor. In Eq. (2), $R^{\mu\nu\sigma\lambda}$ is the Riemann tensor of general relativity and $\tilde{R}_{\mu\nu\sigma\lambda} = \epsilon_{\mu\nu\alpha\beta}R^{\alpha\beta}_{\sigma\lambda}$ is its dual. In both cases ϕ is some scalar field of relevance in the early Universe, such as the inflaton or quintessence. Now, in both cases, there is no parity violation if ϕ is constant in space and time, since then the terms of Eqs. (1) and (2) are total derivatives. Such terms do not contribute to the equations of motion since integration by parts removes them from the action.

In both cases, parity violation leads to a preferred helicity for fluctuations, respectively, in the gauge field for Eq. (1) and in the metric for Eq. (2). This in turn induces parity violation in the correlations between the curvature perturbations and ultimately in the subsequent correlations between density fluctuations, which seed the formation of the galaxies we may observe in surveys of the late-time Universe.

Searching for parity violation with the 4PCF.—To search for parity violation we separate the parity-conserving and parity-violating components of the correlation function between fractional density fluctuations $\delta(\mathbf{r}) \equiv \rho(\mathbf{r})/\bar{\rho} - 1$ at locations $\mathbf{r}_i, i = 0,\ 1,\ 2,\ 3,$ where $\rho(\mathbf{r})$ is the density and $\bar{\rho}$ its average. By homogeneity one of the positions can be taken as the origin. Without loss of generality we thus set $\mathbf{r}_0 = 0$ so that the 4PCF is a function of three vectors; we denote it $\zeta(\mathbf{r}_1, \mathbf{r}_2, \mathbf{r}_3)$. By isotropy ζ must be invariant under simultaneous rotation of $\mathbf{r}_1$, $\mathbf{r}_2$, and $\mathbf{r}_3$. The 4PCF thus depends on three radial distances r_1, r_2, r_3 and the collection of angles defining directions $\hat{\mathbf{r}}_1, \hat{\mathbf{r}}_2, \hat{\mathbf{r}}_3$. One can straightforwardly show that when the 4PCF is averaged over all orientations with respect to the line of sight, redshift-space distortions (RSD) [20] do not produce any parity-breaking signal.

In previous work [8] two of us showed how to construct a complete set of isotropic basis functions of an arbitrary number of unit vectors; for three (which describe a 4PCF),

$$\mathcal{P}_{\ell_1\ell_2\ell_3}(\hat{\mathbf{r}}_1, \hat{\mathbf{r}}_2, \hat{\mathbf{r}}_3) = (-1)^{\ell_1+\ell_2+\ell_3} \sum_{m_1,m_2,m_3} \begin{pmatrix} \ell_1 & \ell_2 & \ell_3 \\ m_1 & m_2 & m_3 \end{pmatrix} \times Y_{\ell_1 m_1}(\hat{\mathbf{r}}_1) Y_{\ell_2 m_2}(\hat{\mathbf{r}}_2) Y_{\ell_3 m_3}(\hat{\mathbf{r}}_3), \tag{3}$$

where the matrix is a Wigner $3j$ symbol. To complete the specification of the basis functions we label the r_i by the ordering $r_1 \le r_2 \le r_3$. Thus (ℓ_1, m_1) corresponds to the shortest of the r_i, and so on. The triangular inequalities, $|\ell_1 - \ell_2| < \ell_3 < \ell_1 + \ell_2$, are enforced by the $3j$ symbol. The parity of the overall state is odd if the sum of the ℓ_i is odd.

It follows from the properties of the spherical harmonics and the Wigner $3j$ symbols that

$$\mathcal{P}_{\ell_1\ell_2\ell_3}(-\hat{\mathbf{r}}_1, -\hat{\mathbf{r}}_2, -\hat{\mathbf{r}}_3) = (-1)^{\ell_1+\ell_2+\ell_3} \mathcal{P}_{\ell_1\ell_2\ell_3}(\hat{\mathbf{r}}_1, \hat{\mathbf{r}}_2, \hat{\mathbf{r}}_3) = \mathcal{P}^*_{\ell_1\ell_2\ell_3}(\hat{\mathbf{r}}_1, \hat{\mathbf{r}}_2, \hat{\mathbf{r}}_3). \tag{4}$$

Consequently, $\mathcal{P}_{\ell_1\ell_2\ell_3}$ is real if $\ell_1 + \ell_2 + \ell_3$ is even and is imaginary if the sum is odd. A variety of useful algebraic relations among the $\mathcal{P}_{\ell_1\ell_2\ell_3}$ are given in Ref. [8].

The 4PCF can be expanded as

$$\zeta(\mathbf{r}_1, \mathbf{r}_2, \mathbf{r}_3) = \sum_{\ell_1\ell_2\ell_3} \mathcal{Z}_{\ell_1\ell_2\ell_3}(r_1, r_2, r_3) \mathcal{P}_{\ell_1\ell_2\ell_3}(\hat{\mathbf{r}}_1, \hat{\mathbf{r}}_2, \hat{\mathbf{r}}_3). \tag{5}$$

It follows from the properties of the $\mathcal{P}_{\ell_1\ell_2\ell_3}$ that $\mathcal{Z}_{\ell_1\ell_2\ell_3}$ is real if $\ell_1 + \ell_2 + \ell_3$ is even and imaginary if the sum is odd. The expansion coefficient $\mathcal{Z}_{\ell_1\ell_2\ell_3}$ is obtained by averaging over the continuous position $\mathbf{x}$ out from which $\mathbf{r}_1$, $\mathbf{r}_2$, $\mathbf{r}_3$ are measured:

$$\mathcal{Z}_{\ell_1\ell_2\ell_3}(r_1, r_2, r_3) = \int \frac{d^3\mathbf{x}}{V} \int d\hat{\mathbf{r}}_1 d\hat{\mathbf{r}}_2 d\hat{\mathbf{r}}_3\, \hat{\zeta}(\mathbf{r}_1, \mathbf{r}_2, \mathbf{r}_3; \mathbf{x}) \times \mathcal{P}^*_{\ell_1\ell_2\ell_3}(\hat{\mathbf{r}}_1, \hat{\mathbf{r}}_2, \hat{\mathbf{r}}_3), \tag{6}$$

where V is the volume over which $\mathbf{x}$ ranges. In the integrand, $\hat{\zeta}(\mathbf{r}_1, \mathbf{r}_2, \mathbf{r}_3; \mathbf{x})$ is the estimate of the 4PCF obtained by sitting at a point $\mathbf{x}$, i.e., it is $\delta(\mathbf{x})\delta(\mathbf{x} + \mathbf{r}_1)\delta(\mathbf{x} + \mathbf{r}_2)\delta(\mathbf{x} + \mathbf{r}_3)$; we are projecting this estimate onto the basis of $\mathcal{P}_{\ell_1\ell_2\ell_3}$ and then, with $\int d^3\mathbf{x}/V$, averaging over all possible centers $\mathbf{x}$.

The problem of measuring efficiently the large-scale 3PCF in the distribution of galaxies was solved by the technique developed in Refs. [21–23], with extensions to 4PCF and higher by Ref. [24]. We briefly outline the approach here.

In practice we have in place of the continuous distribution of density fluctuations $\delta(\mathbf{r})$ the collection of discrete galaxy locations. As a first step, we choose a galaxy at an absolute position $\mathbf{x}_i$. Next, we bin the relative distances of its neighbors into spherical shells which we denote by r_j^b. We then expand the angular dependence in each shell in spherical harmonics as

$$\delta(\mathbf{x}_i, r_j^b, \hat{\mathbf{r}}) = \sum_{\ell,m} a_{\ell m}(\mathbf{x}_i, r_j^b) Y_{\ell m}(\hat{\mathbf{r}}), \tag{7}$$

where

$$a_{\ell m}(\mathbf{x}_i, r_j^b) = \sum_\alpha Y^*_{\ell m}(\hat{\mathbf{r}}_\alpha). \tag{8}$$

The summation is over galaxies $\alpha = 1, 2, \ldots$ in the radial bin r_j^b surrounding the galaxy at $\mathbf{x}_i$.

Using Eq. (7) for $\delta(\mathbf{x}_i, r_j^b, \hat{\mathbf{r}})$ and forming the product indicated by $\hat{\zeta}$ [defined below Eq. (6)], we then project onto the basis of $P_{\ell_1\ell_2\ell_3}$ [see Eq. (3)] and average over $\mathbf{x}_i$ [the discrete analog of $\int d^3\mathbf{x}/V$ in Eq. (6)]. The result is

$$\mathcal{Z}_{\ell_1\ell_2\ell_3}(r_1^b, r_2^b, r_3^b) = (-1)^{\ell_1+\ell_2+\ell_3} \sum_{m_1 m_2 m_3} \begin{pmatrix} \ell_1 & \ell_2 & \ell_3 \\ m_1 & m_2 & m_3 \end{pmatrix} \times \mathcal{A}_{\ell_1 m_1, \ell_2 m_2, \ell_3 m_3}(r_1^b, r_2^b, r_3^b), \quad (9)$$

where we have defined

$$\mathcal{A}_{\ell_1 m_1, \ell_2 m_2, \ell_3 m_3}(r_1^b, r_2^b, r_3^b) = \frac{1}{N_g} \sum_{i=1}^{N_g} a_{\ell_1 m_1}(\mathbf{x}_i, r_1^b) a_{\ell_2 m_2}(\mathbf{x}_i, r_2^b) a_{\ell_3 m_3}(\mathbf{x}_i, r_3^b), \quad (10)$$

and there are N_g galaxies in the survey.

The observables are the $\mathcal{Z}_{\ell_1\ell_2\ell_3}(r_1^b, r_2^b, r_3^b)$. Each is specified by three integers constrained by the triangular inequalities, and by three radial bins. *A priori* there is no preferred scale for searching parity violation. Searches where each tetrahedron side is of the order of a few megaparsecs to 100 or 200 Mpc seem reasonable. With $\ell_{\max} = 4$, a bin width of 10 Mpc, a maximal side length r_j^b of 200 Mpc, and excluding coefficients with any two radial bins identical (to eliminate the shortest-distance correlations), there are 2760 $\mathcal{Z}_{\ell_1\ell_2\ell_3}(r_1^b, r_2^b, r_3^b)$ amplitudes.

More daunting is the challenge of determining the covariance matrix among so many observables. An analytic expression for the covariance matrix can be obtained by assuming a Gaussian random density field when evaluating the appropriate expectation value of eight density fluctuations [25]. This offers a smooth, invertible template, which can then be calibrated using a reasonably modest number of mock catalogs. An analytical covariance template can be used to mitigate the sampling fluctuations that occur when the covariance is simply drawn from a number of mock catalogs [26,27], which on their own could lead to a covariance matrix that fails even to be positive semidefinite [28].

Detectability estimate.—We now consider the prospects for constraining parity violation with the method proposed herein, in the context of a simplified signal. We first determine the optimal number of degrees of freedom to use in such an analysis and then ask what level of parity violation could be detected at 5σ with data from the BOSS CMASS sample [29]. We then evaluate the potential impact of underestimating the covariance matrix. Finally, we make a full Fisher forecast for current and future datasets such as BOSS and DESI, using a single-parameter representation of the signal.

Optimal analysis, detection threshold, and impact of covariance underestimation.—To explore the possibility of detection, we need both a covariance matrix to incorporate statistical fluctuations and a representation of the signal. Rather than consider any of the theoretical models that can produce parity violation, here we seek to make a forecast that is sensitive to any parity violation regardless of its underlying source. To do this, we use a χ^2 test.

In the absence of a physical model, we take guidance from a covariance matrix that is derived from an analytic template that assumes the galaxy density fluctuation field is Gaussian random [25]. The effect of shot noise, a consequence of the discreteness of the galaxies, is incorporated in the covariance matrix using the parameters of the BOSS CMASS dataset, as described more completely below.

The eigenvalues λ_i of the covariance matrix give the variance on each of the statistically independent eigenvectors and we order them $\lambda_1 \leq \lambda_2 \ldots$, i.e., from "best" to "worst" in precision. Our simple representation of the signal assigns the same amplitude ζ (up to an irrelevant sign and ignoring the irrelevant factor i in the parity-odd amplitudes) in each of the eigenvectors that diagonalize the covariance matrix. We take this uniform ("Laplacian ignorance" [30]) prior for the independent amplitudes since without a physical model we lack a basis for distinguishing among them.

If we use only the N eigenvectors with the highest precision (smallest λ_i), then on average

$$\langle \chi^2 \rangle = \sum_{i=1}^{N} (1 + \zeta^2 \lambda_i^{-1}) = N + \zeta^2 \sum_{i=1}^{N} \lambda_i^{-1} \equiv N + \Delta\chi^2, \quad (11)$$

where the last line defines $\Delta\chi^2$, the mean excess χ^2 relative to that under the null hypothesis of no signal. We note that the eigenvalues of the inverse covariance scale as the survey volume used to evaluate it [25], and hence so does $\Delta\chi^2$.

The standard deviation of the χ^2 distribution for N degrees of freedom is $\sqrt{2N}$, and so the average detection significance S in units of σ_{χ^2} is roughly

$$S \approx \frac{\Delta\chi^2}{\sqrt{2N}} = \zeta^2 (2N)^{-1/2} \sum_{i=1}^{N} \lambda_i^{-1}. \quad (12)$$

Rather than using all available eigenvectors we maximize the significance S in Eq. (12) by varying the number N of eigenvectors; we find

$$\lambda_N^{-1} = \frac{1}{2N} \sum_{i=1}^{N} \lambda_i^{-1}. \quad (13)$$

The optimal N is thus when the next value of λ_i^{-1} is half the mean of the preceding λ_i^{-1}. See Fig. 1, which shows the optimal $N = 269$ for the BOSS CMASS data. For this calculation, in our initial covariance, we used ten radial bins and all $\ell_i \leq \ell_{\max} = 4$, leading to 2760 total degrees of freedom for the parity-odd 4PCF; the $N = 269$ eigenvectors then represent a down-selection among linear combinations of the initial isotropic basis coefficients of Eqs. (9) and (10). We use the number density of BOSS luminous red galaxies (LRGs), $\bar{n} = 2.2 \times 10^{-4}\,(h^{-1}\,\mathrm{Mpc})^{-3}$ (from BOSS DR16 CMASS, ~800 000 objects) for $z = 0.43$–0.7 and

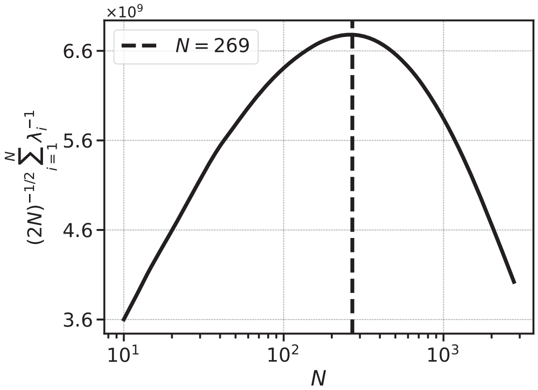

FIG. 1. Partial sums of the first N eigenvalues λ_i^{-1} of the inverse covariance, divided by $\sqrt{2N}$. The detection significance if a signal is uniform in each eigenvector will always be *proportional to* this curve [ζ^2 times it; see Eq. (12)]. The same method of optimizing the number of eigenvectors could be employed with an explicit model for the signal in each eigenvector. Here, to evaluate the covariance, we used the number density, galaxy bias, etc. for BOSS CMASS, with values given in the caption of Fig. 2.

sky fraction implied by 9376 deg^2 [31]. We input a nonlinear matter power spectrum scaled by the galaxy bias and linear RSD [32] and use an effective volume following Ref. [33]. We emphasize that if the survey volume is scaled up while all other parameters are held constant, the significance increases linearly with it and not as its square root.

We now ask to what level of parity violation a 5σ detection in BOSS would correspond. Inverting Eq. (12) with $S \equiv 5$, $N = 269$, we find, using Fig. 1, $\zeta = 2.7 \times 10^{-5}$. We may compare this value to the leading parity-even 4PCF amplitudes in the Gaussian random field approximation. Since the even and odd basis functions have the same normalization convention, the magnitudes are directly comparable. We expect the parity-even amplitudes to be of order 10^{-2}, roughly the 2PCF squared. Thus parity violation of a few parts per mille relative to the even 4PCF is detectable at 5σ in BOSS CMASS under the assumptions made above.

Underestimating the covariance matrix could lead to a spurious detection of apparent parity violation. Inadvertently taking it to be $(1-\epsilon)$ of its true value would on average produce a mistaken $\langle \Delta\chi^2 \rangle = \epsilon N/(1-\epsilon)$ since this would result in $\langle \chi^2 \rangle = \sum_i (\zeta^2 + \lambda_i)/[(1-\epsilon)\lambda_i] = N/(1-\epsilon)$ if $\zeta = 0$ [Eq. (12)]. The apparent significance would then be $S = \epsilon\sqrt{N/2}/(1-\epsilon)$. To produce a spurious 5σ detection on 200 degrees of freedom would require an underestimate of the covariance by 33%; for the same on 400 degrees of freedom, by 26%. To guard against this, the analytic covariance matrix can be calibrated against an empirical covariance derived from averaging over many mock catalogs from simulations [25]. Increasing the survey volume with number density and galaxy population held fixed would decrease the covariance matrix, but if the same fractional error ϵ were made, the size of the spurious detection would be unchanged. In contrast, if the signal is real, then its significance will dramatically increase with a future survey, scaling as volume if a fixed number of degrees of freedom are used for the analysis [see remark below Eqs. (11) and (12)].

Power of current and future datasets.—We now compare of the power of the BOSS CMASS data with that which will be available for the DESI surveys of LRGs and emission line galaxies (ELGs). A basic assumption here is that different galaxy populations trace a common primordial signal. To enable the comparison between different samples, we scale the signal from BOSS to DESI and account for the difference in shot noise.

Scaling of signal.—To enable comparison between samples, we take a fixed amplitude ζ_0 (constant) at all the eigenvectors, such that the signal in BOSS CMASS would manifest at 5σ, and then scale to other samples as

$$\zeta = \frac{b_1^4 D^4(z)\langle (1+\beta\mu^2)^4 \rangle}{(b_1^4 D^4(z)\langle (1+\beta\mu^2)^4 \rangle)|_{\mathrm{BOSS}}} \zeta_0. \tag{14}$$

This scaling includes linear bias b_1, growth factor $D(z)$, and RSD enhancement due to the linear Kaiser factor. Angle brackets denote averaging over angle to the line of sight, with μ its cosine, and $\beta \equiv (d \ln D/d \ln a)/b_1$, with a the scale factor. The denominator is evaluated at BOSS CMASS parameters. This scaling captures how different galaxy populations would trace a common primordial signal.

Details of covariance.—For each sample, we also scale the power spectrum entering the covariance appropriately by these factors, and in the covariance use the number density for the given class. We note that since the covariance includes both power spectrum and shot noise [25], while the scaled signal does not depend on the latter, the scaling applied to the signal will not cancel with that of the power spectrum in the covariance; thus the detection significance's dependence on galaxy bias, growth rate, etc. is nontrivial.

To obtain the $\bar{n}$ used in the covariance, we integrate $n(z)$, the number density as a function of redshift, over each survey's redshift range. For CMASS we take this from the actual survey data [31] and for DESI from Ref. [34]. The effective volume V_{eff} we use is also evaluated based on these $n(z)$, following Ref. [33].

We explore the impact of variation in number density while holding number of objects in each class fixed; this reflects a fixed amount of observing time for a given sample. This is motivated by possible opportunities to use the DESI instrument for a subsequent survey (DESI-II). Furthermore, future missions beyond DESI such as SpecTel [35] or MegaMapper [36] could produce samples with number densities much higher, as presented toward the

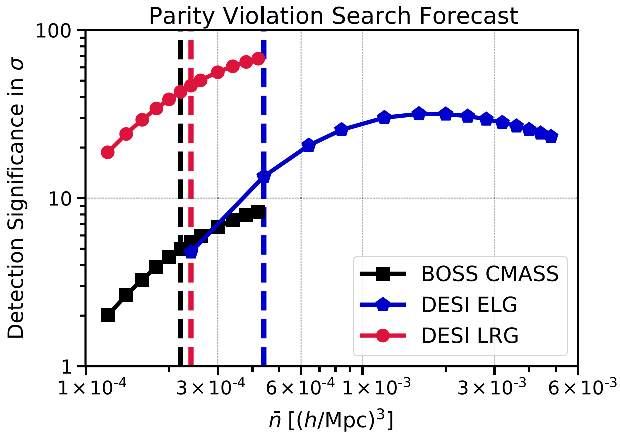

FIG. 2. Forecast detection significances for BOSS and DESI with $N = 269$ eigenvectors (see Fig. 1), computed via Eq. (12). We have set our baseline signal so that BOSS CMASS would have a 5σ detection; thus this plot shows how well a DESI-like survey could follow up a detection were one made in BOSS. For each class, we hold number of objects constant (BOSS CMASS, 0.8 M; DESI LRG, 7.2 M; DESI ELG, 16 M) and vary the number density $\bar{n}$ around the fiducial values (vertical dashed lines); this in turn implies varying the nominal volume. While increased density reduces the shot noise, decreased volume increases the covariance so that the curves eventually turn over. Future experiments with greater numbers of observed galaxies would have analogous curves at higher overall amplitudes but with the same shape. The nominal densities are indicated by the vertical dashed lines. The corresponding effective volumes in $[\mathrm{Gpc}/h]^3$ are $V_{\mathrm{LRG}}^{\mathrm{BOSS}} = 1.6$, $V_{\mathrm{LRG}}^{\mathrm{DESI}} = 12.4$, $V_{\mathrm{ELG}}^{\mathrm{DESI}} = 17.3$. We use the galaxy biases from [37]: $b_{\mathrm{LRG}}(z = 0.7) = 2.4$ for both DESI and BOSS; $b_{\mathrm{ELG}}(z = 1.1) = 1.4$.

rightmost region of Fig. 2. We defer full exploration of survey strategy for a parity-violation search to future work.

Optimal number of eigenvectors N.—We evaluate all forecasts at the optimal $N = 269$ found for BOSS CMASS above. Numerical studies showed that the results for all BOSS and DESI samples, and over a range in number density, would be insensitive to changes of N within $\pm 20\%$. We thus set $N = 269$ for all classes in Fig. 2.

Discussion.—Overall we see that the BOSS LRG to DESI LRG improvement is roughly in the ratio of effective volumes V_{eff}. While the change in volume was not the only modification of the covariance matrix going from BOSS to DESI, it was the dominant effect and the result is in accord with the expectation from Eqs. (11) and (12). For DESI, we find that the LRGs outperform the ELGs, mainly due to the difference in galaxy bias.

The work of R. N. C. was supported in part by the Director, Office of Science, Office of High Energy Physics, of the U.S. Department of Energy under Contract No. DE-AC02-05CH11231. Z. S. gratefully acknowledges support from the National Aeronautics and Space Administration through Einstein Postdoctoral Fellowship Award No. PF7-180167 issued by the Chandra Xray Observatory Center, which is operated by the Smithsonian Astrophysical Observatory for and on behalf of the National Aeronautics Space Administration under Contract No. NAS8-03060. Z. S. also acknowledges support from a Chamberlain Fellowship at Lawrence Berkeley National Laboratory (held previously to the Einstein Fellowship) and from the Berkeley Center for Cosmological Physics. J. H. has received funding from the European Union's Horizon 2020 research and innovation program under the Marie Skłodowska-Curie Grant Agreement No 101025187.

Note added.—Subsequent to the initial submission of this paper, data analyses using the technique proposed here were done by Hou *et al.* [38] and by Philcox [39].

*rncahn@lbl.gov

[1] C. S. Wu, E. Ambler, R. W. Hayward, D. D. Hoppes, and R. P. Hudson, Phys. Rev. **105**, 1413 (1957).
[2] R. L. Garwin, L. M. Lederman, and M. Weinrich, Phys. Rev. **105**, 1415 (1957).
[3] J. I. Friedman and V. L. Telegdi, Phys. Rev. **105**, 1681 (1957).
[4] A. D. Sakharov, Sov. JETP Lett. **5**, 24 (1967).
[5] A. Riotto and M. Trodden, Annu. Rev. Nucl. Part. Sci. **49**, 35 (1999).
[6] J. H. Christenson, J. W. Cronin, V. L. Fitch, and R. Turlay, Phys. Rev. Lett. **13**, 138 (1964).
[7] D. P. Glavin, A. S. Burton, J. E. Elsila, J. C. Aponte, and J. P. Dworkin, Chem. Rev. **120**, 4660 (2020).
[8] R. N. Cahn and Z. Slepian, arXiv:2010.14418.
[9] A. Lue, L. Wang, and M. Kamionkowski, Phys. Rev. Lett. **83**, 1506 (1999).
[10] S. Alexander and N. Yunes, Phys. Rep. **480**, 1 (2009).
[11] M. Kamionkowski and T. Souradeep, Phys. Rev. D **83**, 027301 (2011).
[12] D. Jeong and M. Kamionkowski, Phys. Rev. Lett. **108**, 251301 (2012), This reference considers both CMB and large-scale structure.
[13] N. Bartolo, S. Matarrese, M. Peloso, and A. Ricciardone, Phys. Rev. D **87**, 023504 (2013).
[14] N. Bartolo, S. Matarrese, M. Peloso, and M. Shiraishi, J. Cosmol. Astropart. Phys. 01 (2015) 027.
[15] M. Shiraishi, Phys. Rev. D **94**, 083503 (2016).
[16] N. Bartolo and G. Orlando, J. Cosmol. Astropart. Phys. 07 (2017) 034.
[17] Y. Minami and E. Komatsu, Phys. Rev. Lett. **125**, 221301 (2020).
[18] K. W. Masui, U.-L. Pen, and N. Turok, Phys. Rev. Lett. **118**, 221301 (2017).
[19] S. M. Carroll, Phys. Rev. Lett. **81**, 3067 (1998).
[20] A. J. S. Hamilton, Linear redshift distortions: A review, in *The Evolving Universe*, edited by D. Hamilton (Springer, New York, 1998), Vol. 231, p. 185.

[21] Z. Slepian and D. J. Eisenstein, Mon. Not. R. Astron. Soc. **454**, 4142 (2015).

[22] Z. Slepian and D. J. Eisenstein, Mon. Not. R. Astron. Soc. **455**, L31 (2015).

[23] S. K. N. Portillo, Z. Slepian, B. Burkhart, S. Kahraman, and D. P. Finkbeiner, Astrophys. J. **862**, 119 (2018).

[24] O. H. E. Philcox, Z. Slepian, J. Hou, C. Warner, R. N. Cahn, and D. J. Eisenstein, Mon. Not. R. Astron. Soc. **509**, 2457 (2021).

[25] J. Hou, R. N. Cahn, O. H. E. Philcox, and Z. Slepian, Phys. Rev. D **106**, 043515 (2022).

[26] R. Scoccimarro, Astrophys. J. **544**, 597 (2000).

[27] B. Joachimi, Mon. Not. R. Astron. Soc. **466**, L83 (2016).

[28] O. P. Van Driel, Psychometrika **43**, 225 (1978).

[29] S. Alam, F. D. Albareti, C. A. Prieto, F. Anders, S. F. Anderson, T. Anderton, B. H. Andrews, E. Armengaud, E. Aubourg, S. Bailey *et al.*, Astrophys. J. Suppl. Ser. **219**, 12 (2015).

[30] P. S. Laplace, *A Philosophical Essay on Probabilities* (John Wiley and Sons Limited, New York, 1902).

[31] B. Reid, S. Ho, N. Padmanabhan, W. J. Percival, J. Tinker, R. Tojeiro, M. White, D. J. Eisenstein, C. Maraston, A. J. Ross *et al.*, Mon. Not. R. Astron. Soc. **455**, 1553 (2016).

[32] N. Kaiser, Mon. Not. R. Astron. Soc. **227**, 1 (1987).

[33] M. Tegmark, Phys. Rev. Lett. **79**, 3806 (1997).

[34] K. Dawson, A. Hearin, K. Heitmann, M. Ishak, J. Ulf Lange, M. White, and R. Zhou, arXiv:2203.07291.

[35] R. Ellis and K. Dawson, Bull. Am. Astron. Soc. **51**, 45 (2019).

[36] D. Schlegel, J. A. Kollmeier, and S. Ferraro, Bull. Am. Astron. Soc. **51**, 229 (2019).

[37] A. Aghamousa *et al.* (DESI Collaboration), arXiv:1611.00036.

[38] J. Hou, Z. Slepian, and R. N. Cahn, arXiv:2206.03625.

[39] O. H. E. Philcox, Phys. Rev. D **106**, 063501 (2022).